

# DARK MATTER SELF-INTERACTIONS FROM THE INTERNAL DYNAMICS OF DWARF SPHEROIDALS

MAURO VALLI

INFN, Sezione di Roma, P.le A. Moro 2, I-00185 Roma, Italy

HAI-BO YU

Department of Physics and Astronomy, University of California, Riverside, California 92521, USA

## ABSTRACT

Using the dataset of stellar kinematics for the brightest Milky Way dwarf spheroidal galaxies, we underpin the goodness of the self-interacting dark matter (SIDM) proposal as a solution to the “too-big-to-fail” problem through a detailed fit of the stellar velocity dispersion profiles. The kinematic data are consistent with SIDM if we allow for spatially varying stellar orbital anisotropies. We provide the first data-driven estimate for the SIDM cross-section per unit mass probed by these galaxies, pointing to  $\sigma/m \sim 0.5 - 3 \text{ cm}^2\text{g}^{-1}$ , in good agreement with recent estimates from the study of the dynamics in spiral galaxies. Our results well match the trends previously observed in pure SIDM N-body simulations. The analysis in this work outlines a complementary approach to simulations in testing SIDM with astrophysical observations.

*Keywords:* dark matter — galaxies: dwarf — galaxies: halos

## 1. INTRODUCTION.

Within a possible small-scale crisis for the cold dark matter (CDM) paradigm (see, e.g., (Bullock & Boylan-Kolchin 2017; Tulin & Yu 2017)), dwarf spheroidal galaxies (dSphs) of the Milky Way (MW) supply today the toughest challenges, with long-standing problems as the “missing satellites” (MS) (Klypin et al. 1999; Moore et al. 1999) and the “too-big-to-fail” (TBTF) (Boylan-Kolchin et al. 2011, 2012). The MS puzzle stems from the thousands of sub-halos predicted by pure CDM simulations in MW-sized boxes in opposition to the tens of satellites observed nearby our Galaxy. The TBTF problem stands out as the mismatch between the enclosed mass at the half-light radius (Walker et al. 2009; Wolf et al. 2010) of the brightest MW dSphs and the dynamical properties of the most massive sub-halos predicted in CDM-only simulations. Recent N-body hydrodynamical studies of the Local Group environment (Sawala et al. 2016; Wetzel et al. 2016; Fattahi et al. 2016) indicate that re-ionization and star formation histories, and effects of tidal stripping from the host galaxy, play a crucial role for these small-scale controversies. However, low luminosity and lack of gas in dSphs may suggest mild effects from baryonic physics (Ferrero et al. 2012; Peñarrubia et al. 2012; Garrison-Kimmel et al. 2013). Moreover, while the MS puzzle has been ameliorated in the last decade (see Drlica-Wagner et al. (2015) and references therein), the TBTF has been reinforced by the observation of a similar puzzle in the field (Papastergis et al. 2015). Consequently, the TBTF problem may establish a well-motivated link with

beyond CDM scenarios (Vogelsberger et al. 2016).

After almost two decades from the proposal of Spergel & Steinhardt (2000), the self-interacting DM (SIDM) paradigm receives special attention for the CDM small-scale crisis (Tulin & Yu 2017). Indeed, self-interactions of DM particles can thermalize the inner halo, while keeping unaltered CDM predictions at large scales (Vogelsberger et al. 2012; Rocha et al. 2013). The thermalization correlates the DM and baryon distributions in the inner halo (Kaplinghat et al. 2014; Elbert et al. 2015), offering an explanation to the “Diversity problem”, i.e. the observed variety of spiral galaxy rotation curves (Kamada et al. 2017; Creasey et al. 2017). For DM dominated systems, DM self-interactions create a density core, addressing the mass deficit observed in many dwarf galaxies, i.e. the “Core vs Cusp” problem. Being such a system, MW dSphs may be a unique probe of this problem (Battaglia et al. 2008; Walker & Peñarrubia 2011; Amorisco et al. 2012; Agnello et al. 2012; Amorisco et al. 2013), although a definite establishment of it is probably not yet conceived (Strigari et al. 2017).

In this *Letter*, motivated by several hints in favor of a “Core vs Cusp” problem in MW dSphs, we present a detailed study of their internal dynamics within SIDM. We fit the stellar kinematics of these systems using the semi-analytical SIDM halo model of Kaplinghat et al. (2014, 2016), and the N-body information from Vogelsberger et al. (2016). Our final aim is twofold: *i*) assess the goodness of SIDM as a solution of the TBTF; *ii*) obtain the corresponding data-driven estimate of the SIDM cross-

section. In section 2 we present the basics of our Jeans analysis; section 3 collects the details of our fitting procedure; in section 4 and 5 we discuss the original findings of our study, see figure 1–3, table 1. We leave our ending comments to Section 6.

## 2. SIDM – STELLAR JEANS ANALYSIS.

The internal dynamics of MW dSphs is commonly studied exploiting the kinematics of a stellar population of density  $\rho_*$ , in dynamical equilibrium under the gravitational potential governed by DM,  $\Phi_{\text{DM}}$ . For a spherically symmetric steady-state system, the first moment of the collision-less Boltzmann equation for the stellar phase-space distribution takes the form:

$$(\rho_* \sigma_r^2)' + 2\beta(r)\rho_*(r)\sigma_r^2(r) = -\rho_*(r)\Phi_{\text{DM}}', \quad (1)$$

where the prime denotes logarithmic derivative in  $r$ . The stellar orbital anisotropy,  $\beta \equiv 1 - \sigma_t^2/\sigma_r^2$ , measures the deviation from isotropy in the stellar velocity dispersion tensor. Photometric observations of dSph surface brightness constrain  $\rho_*$ . Supplying equation (1) with Poisson’s equation, mass and orbital anisotropy are inferred from line-of-sight (l.o.s.) projected spectroscopic measurements, leading generally to a degeneracy problem (Battaglia et al. 2013).

Turning the attention to the DM profile, the SIDM paradigm provides a semi-analytical halo model based on simple physical grounds. Introducing the DM self-scattering rate as  $\Gamma_{\text{DM}} \equiv \langle \sigma_{\text{DM}} v \rangle \rho / m$ , with velocity averaged cross-section,  $\langle \sigma_{\text{DM}} v \rangle$ , density  $\rho$ , and particle mass  $m$ , we can define the scale  $r_1$  for which:  $\Gamma_{\text{DM}}|_{r_1} \simeq t_{\text{age}}^{-1}$ , being  $t_{\text{age}}$  the typical age of the system. As illustrated in Kaplinghat et al. (2014, 2016),  $r_1$  sets a transition a regime of isothermal gas with pressure  $p \propto \rho$  ( $r \lesssim r_1$ ) to the one of a non-interacting particle ensemble ( $r \gtrsim r_1$ ). For DM dominated systems as MW dSphs, in the inner halo region the SIDM profile is given by:

$$x \ddot{h} + 2\dot{h} = -x \exp[h(x)], \quad \lim_{x \rightarrow 0} h(x) = 0, \quad \lim_{x \rightarrow 0} \dot{h} = 0, \quad (2)$$

where upper-dots denote derivatives in  $x$ , with  $x \equiv \sqrt{4\pi G_N \rho_0} r / \sigma_0$  and  $h \equiv \ln(\rho/\rho_0)$ . The physical halo from equation (2) is an isothermal cored profile involving the one-dimensional DM velocity dispersion,  $\sigma_0$ , defining the SIDM isothermal gas law, and the central density,  $\rho_0$ . The solution of equation (2) is then matched at  $r_1$  to the Navarro-Frenk-White (NFW) model (Navarro et al. 1997). We note that an estimate of the self-scattering cross-section can be obtained by  $\sigma_{\text{DM}} \simeq \langle \sigma_{\text{DM}} v \rangle / \langle v \rangle$ , using  $\langle v \rangle \simeq 4\sigma_0/\sqrt{\pi}$  under Maxwellian approximation, supported by DM self-interactions.

## 3. SETUP AND FITTING PROCEDURE.

The brightest MW dSphs may be regarded as relaxed systems, with negligible tidal disruption and small ellipticities (Battaglia et al. 2013). Therefore, these objects are fairly good candidates for the Jeans analysis of the previous section. We adopt here the spectroscopic

dataset for the “classical” dSphs elaborated in Geringer-Sameth et al. (2015), which provides an updated set of the stellar kinematics originally presented in Walker et al. (2009). Our analysis is based on the fit to binned l.o.s. velocity dispersion data by means of the likelihood:

$$-2 \ln \mathcal{L} \propto \sum_{i=1}^{N_{\text{bins}}} \left[ \frac{\sigma_{\text{los}}^{(i)} - \sigma_{\text{los}}(R^{(i)})}{\Delta \sigma^{(i)}(R^{(i)})} \right]^2, \quad (3)$$

where  $\Delta \sigma^{(i)}(R^{(i)})$  includes the measured velocity dispersion error summed up in quadrature to the one from data binning, see Bonnavard et al. (2015). Regarding the stellar profile, we adopt heliocentric distances and projected half-light radii,  $R_{1/2}$ , from McConnachie (2012), implementing for  $\rho_*$  the Plummer model.

The novelty of our fitting procedure consists in the inclusion of the information about the circular velocity profile predicted for MW dSphs by pure CDM N-body simulations. As a proxy for the CDM-only potential well in these systems, we exploit the spread in  $V_c(r) = \sqrt{G_N M(r)}/r$  obtained for the CDM simulation in Vogelsberger et al. (2016), encompassing the 15 most massive sub-haloes within a host halo of  $1.6 \times 10^{12} M_\odot$ . Assuming a NFW model with maximum circular velocity  $V_{\text{max}}$  and scale  $R_{\text{max}}$ , we find the outcome of Vogelsberger et al. (2016) to be approximately reproduced by  $\log_{10}(R_{\text{max}}/[\text{kpc}]) = 0.48 + 0.18 \log_{10}(V_{\text{max}}/[\text{km/s}])$ , with 0.2 dex scatter on  $R_{\text{max}}$  for  $V_{\text{max}} \sim 30 - 60$  km/s. We take this relation to hold up to  $\mathcal{O}(10)$  kpc, reasonably the maximum expected extent for a dSph halo, see Geringer-Sameth et al. (2015); Bonnavard et al. (2015). We include this information as a log-Gaussian weight on  $R_{\text{max}}$  while limiting the span on  $V_{\text{max}}$  by requiring  $25 \lesssim V_c(r = 10 \text{ kpc})/[\text{km/s}] \lesssim 60$ . Eventually, to take into account the prediction in Vogelsberger et al. (2016), we find useful to penalize  $(R_{\text{max}}, V_{\text{max}})$  realizations that do not satisfy  $V_c^{\text{NFW}}(r = 0.5 \text{ kpc}) \gtrsim 19$  km/s.

## 4. SIDM VS CDM: BEST-FITS AT HAND.

To start with, we show in figure 1 with dashed light-blue lines the best-fit for l.o.s. velocity dispersion data within the SIDM halo model of Section 2, assuming spatially constant anisotropy. With this setup, radial stellar orbits are forbidden according to An & Evans (2006), i.e.  $\beta \leq 0$ . The best-fit shows net preference for isotropic stellar orbits and highlights tension in the fit between the stellar kinematics and the implemented requirement from cosmology: only Ursa Minor, Draco and Leo I show a satisfactory description of their kinematic data, while satisfying the constraint from Vogelsberger et al. (2016) in  $(R_{\text{max}}, V_{\text{max}})$ .

This motivates us to introduce a more realistic orbital anisotropy modeling as in Baes & Van Hese (2007):

$$\beta(r) = (\beta_0 + \beta_\infty (r/r_\beta)^\eta) / (1 + (r/r_\beta)^\eta), \quad (4)$$

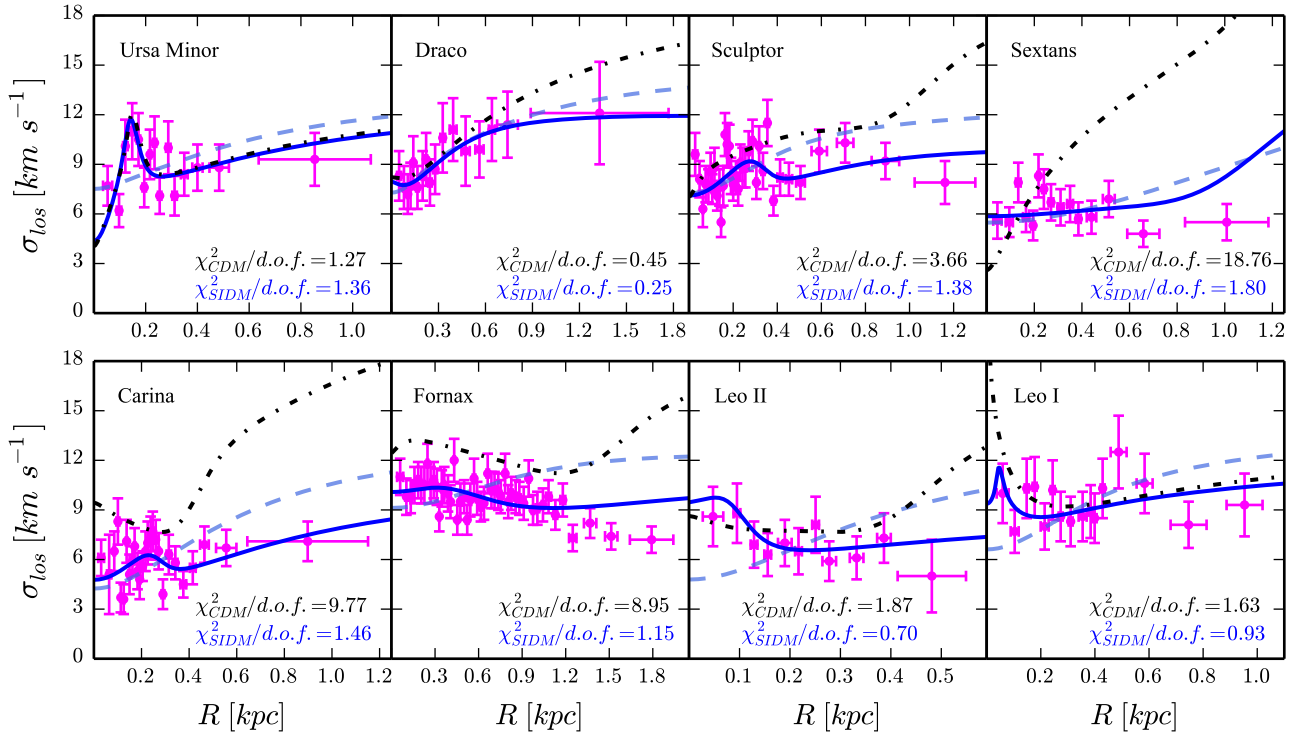


**Figure 1.** Line-of-sight velocity dispersion profiles for the Milky Way “classical” satellites from the joint fit of the stellar kinematics and the cosmological constraint described in the text. Dashed light-blue lines refer to the best-fit SIDM scenario with spatially constant stellar anisotropy. Blue and dot-dashed black lines correspond respectively to the SIDM (7 parameters) and CDM best-fit (6 parameters) cases using the orbital anisotropy function of equation (4). Chi-squared per degrees of freedom (d.o.f.) are reported for both cases.

i.e. a spatial interpolation of the regime of stellar motion at the center, controlled by  $\beta_0$ , and that in the outer region, regulated by  $\beta_\infty$ , with transition scale and slope set by  $r_\beta$  and  $\eta$ . The above generic form for the anisotropy offers also the advantage of reducing biases from restrictive parameterizations of  $\rho_*$  in equation (1). Equipped with equation (4), we perform the SIDM fit varying a total of 7 parameters. We restrict  $\beta_0 \leq 0$  according to An & Evans (2006), and assume  $r_\beta \gtrsim 1$  pc, since smaller scales would not be probed by the kinematic dataset and for  $\beta_\infty \gtrsim 0$  may underly unphysical phase-space densities (see An et al. (2012) and references therein). In figure 1 we show the best-fit for this scenario with blue lines, reporting the reduced chi-squared, scattered around unity. We conclude that radial dependence of the orbital anisotropy allows to find an overall good fit of dSph kinematics, while  $(R_{\max}, V_{\max})$  pairs obtained respect the cosmological picture drawn by CDM N-body analyses. We observe a general trend for the best-fit anisotropy profile corresponding to a sharp ( $\eta \gtrsim 5$ ) transition from  $\beta_0 \simeq 0$  to  $\beta_\infty \simeq 1$  at  $r_\beta \lesssim R_{1/2}$ . The only exception to this is provided by Sextans, where circular-like orbits are preferred in the outer region once we realistically require  $r_1 \lesssim 30$  kpc.

Finally, we perform a direct comparison of the 7-

parameter SIDM fit against the 6-parameter one obtained describing the DM halo with the NFW model. The best-fit result for the latter case is depicted in figure 1 with dot-dashed black lines. Despite the quite generic parametrization in equation (4), stellar kinematics for five of the eight objects is badly reproduced in virtue of the cosmological condition dictated by N-body simulations. We quantify this tension reporting the reduced chi-squared also for this case. We remark that the observed discrepancy represents the essence of the TBTF problem: figure 1 captures the SIDM proposal as a compelling potential solution to this puzzle.

## 5. DATA-DRIVEN ESTIMATE OF THE SIDM CROSS-SECTION IN MW DWARFS.

We perform then a Bayesian fit according to the setup described in section 3. We use the public package *emcee* of Foreman-Mackey et al. (2013), using the affine-invariant ensemble sampler algorithm of Goodman & Weare (2010). We assign log-flat priors as  $-2 \leq \log_{10}(\sigma_0/[\text{km/s}]) \leq 2$ ,  $-3 \leq \log_{10}(\rho_0/[\text{km/s}]) \leq 3$ ,  $-2.5 \leq \log_{10}(r_{1,\beta}/[\text{kpc}]) \leq 1.5$ , while flatly distributing  $1 \leq \eta \leq 10$ ,  $0 < 2^{\beta_0} \leq 1$ ,  $0 < 2^{\beta_\infty} \leq 2^1$ . For each galaxy we run 280 walkers for 3300 steps. We remove one

<sup>1</sup> Posterior for  $\beta_\infty$  in Sextans has two separated modes. We focus on the one yielding  $r_1 \leq 10^{1.5}$  kpc, restricting to  $0 < 2^{\beta_\infty} \leq 1$ .

**Table 1.** Mode and 68% highest density interval of the posterior distribution of SIDM parameters,  $\sigma_0$  [km/s],  $\rho_0$  [ $10^7 M_\odot/\text{kpc}^3$ ],  $r_1$  [kpc], and of orbital anisotropy ones,  $r_\beta$  [kpc],  $\eta$ ,  $\beta_0$ ,  $\beta_\infty$ . Same statistics is also reported for the SIDM averaged self-scattering cross-section per unit mass,  $\langle\sigma v\rangle/m$  [ $\text{cm}^2/\text{g}$ ], and velocity,  $\langle v\rangle$  [km/s].

<i>dSph</i>	$\sigma_0$	$\rho_0$	$r_1$	$r_\beta$	$\eta$	$\beta_0$	$\beta_\infty$	$\langle\sigma v\rangle/m$	$\langle v\rangle$
Ursa Minor	$15.0^{+6.0}_{-2.4}$	$11.9^{+9.3}_{-3.3}$	$0.43^{+0.66}_{-0.41}$	$1.08^{+0.62}_{-1.05} \times 10^{-1}$	$9.9^{+0.1}_{-5.2}$	$-0.2^{+0.2}_{-24} \times 10^{-1}$	$0.77^{+0.09}_{-0.22}$	$9.4^{+16}_{-9.2}$	$33.8^{+14}_{-5.5}$
Draco	$19.7^{+5.5}_{-4.3}$	$8.8^{+4.4}_{-1.9}$	$0.9^{+3.9}_{-0.8}$	$3.0^{+53}_{-0.0} \times 10^{-3}$	$6.7^{+0.4}_{-5.6}$	$-0.2^{+0.2}_{-16} \times 10^{-1}$	$0.54^{+0.20}_{-0.25}$	$34^{+450}_{-6}$	$44.4^{+12}_{-9.7}$
Sculptor	$18.4^{+2.1}_{-0.9}$	$6.1^{+0.6}_{-1.0}$	$1.7^{+3.5}_{-0.3}$	$1.7^{+3.5}_{-0.3}$	$1.6^{+5.1}_{-0.4}$	$-0.2^{+0.2}_{-19} \times 10^{-2}$	$0.80^{+0.06}_{-0.10}$	$67^{+740}_{-34}$	$41.5^{+4.8}_{-2.0}$
Sextans	$27.8^{+4.2}_{-3.6}$	$1.14^{+0.28}_{-0.32}$	$11.0^{+5.2}_{-3.4}$	$1.34^{+0.37}_{-0.41}$	$9.9^{+0.1}_{-3.3}$	$-0.1^{+0.01}_{-9.3} \times 10^{-2}$	$0.0^{+0.0}_{-10}$	$1442^{+2002}_{-938}$	$62.8^{+9.5}_{-8.1}$
Carina	$21.3^{+3.9}_{-3.6}$	$2.56^{+0.46}_{-0.35}$	$4.0^{+4.8}_{-0.6}$	$3.0^{+72}_{-0.0} \times 10^{-3}$	$1.7^{+5.3}_{-0.7}$	$-0.1^{+0.1}_{-16} \times 10^{-1}$	$0.70^{+0.13}_{-0.08}$	$315^{+1311}_{-175}$	$48.2^{+8.7}_{-8.2}$
Fornax	$23.9^{+1.2}_{-1.3}$	$1.11^{+0.12}_{-0.08}$	$10.9^{+1.4}_{-1.7}$	$0.56^{+0.01}_{-0.20}$	$2.74^{+0.89}_{-0.56}$	$-0.1^{+0.1}_{-3.2} \times 10^{-1}$	$0.89^{+0.03}_{-0.03}$	$2116^{+861}_{-567}$	$54.0^{+2.8}_{-3.0}$
Leo II	$18.5^{+8.3}_{-2.4}$	$6.3^{+2.8}_{-1.3}$	$1.2^{+5.2}_{-0.6}$	$3.0^{+45}_{-0.0} \times 10^{-3}$	$9.9^{+0.1}_{-5.6}$	$-0.0^{+0.0}_{-2.3}$	$0.81^{+0.07}_{-0.10}$	$25^{+677}_{-24}$	$41.8^{+19}_{-5.4}$
Leo I	$18.8^{+2.8}_{-3.2}$	$8.5^{+3.9}_{-1.9}$	$1.0^{+1.9}_{-0.8}$	$3.0^{+4.6}_{-0.0} \times 10^{-3}$	$9.8^{+0.2}_{-8.4}$	$-0.1^{+0.1}_{-20} \times 10^{-1}$	$0.73^{+0.10}_{-0.17}$	$18.2^{+142}_{-17.4}$	$42.3^{+6.2}_{-7.2}$

third of the sampler for the burn-in and check sampler convergence estimating both mean acceptance fraction and autocorrelation length for the fitted parameters.

For each dSph we collect in table 1 mode and 68% highest posterior density (h.p.d.) interval of the marginalized distribution for the 7 fitted parameters. The best-fit point in figure 1 always lies within 68% h.p.d. of parameters posterior. We identify Sculptor, Sextans and Fornax to be the most representative cases for the anisotropy profile highlighted in section 4. In figure 2, we show the typical spread on the SIDM circular velocity profile for each dSph computing the 10-th and 90-th percentile of  $V_c$  posterior distribution at different radii. In the outer region, we observe remarkable agreement with the CDM-only output from Vogelsberger et al. (2016), represented by the gray band. In the inner region, we find a satisfactory match to dSph half-light mass estimator originally proposed in Wolf et al. (2010). Colored squares represent nominal values for  $V_{1/2} \simeq \sqrt{3 \langle \sigma_{los}^2 \rangle}$ , estimated here from the fit to stellar kinematics with constant  $\sigma_{los}$  (Ullio & Valli 2016), while error bars are conformed to the recent assessment in Fattahi et al. (2016). Figure 2 reinforces the SIDM proposal as a promising solution to the TBTF, despite non-negligible theoretical bias in the mass estimator for spatially dependent radial anisotropies (Ullio & Valli 2016). A detailed comparison against kinematic data, see figure 1, remains indeed significantly informative.

We eventually exploit the condition  $\Gamma_{\text{DM}}|_{r_1} \simeq t_{\text{age}}^{-1}$  to provide a data-driven estimate of the SIDM cross-section. We marginalize over dSph age with flat prior  $8 \leq t_{\text{age}}/[\text{Gyr}] \leq 12$ , according to observational indicators suggesting MW dSphs to be early-type galaxies (McConnachie 2012). We collect our extraction of the averaged cross-section per unit mass and particle velocity in the last two columns of table 1. In figure 3, we directly

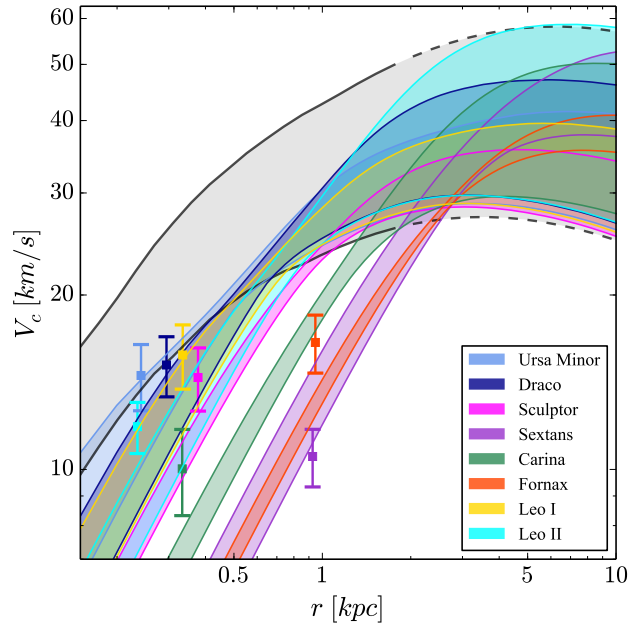


**Figure 2.** Circular velocity profiles extracted from the Bayesian fit discussed in the text. Colored band for each dwarf includes the 10-th and 90-th percentile of  $V_c$  posterior distribution. Colored points indicate dSph mass estimator at half-light radius. Gray band encompasses the most-massive 15 sub-halos from CDM-only simulation of Vogelsberger et al. (2016), and it is extrapolated here above  $\sim 2$  kpc with the NFW model (dashed lines).

inspect the posterior distribution of DM self-scattering cross-section per unit mass. We find Ursa Minor, Draco and Leo I probing cross-sections  $\sim 0.5 \text{ cm}^2/\text{g}^{-1}$ , while Leo II, Sculptor and Carina compatible with  $\sigma/m \sim \mathcal{O}(1) \text{ cm}^2/\text{g}^{-1}$  within the 68% h.p.d.. We identify Fornax and Sextans as “outliers” favoring large cross-section values: within the 99.7% h.p.d. Sextans yields  $\sigma/m \gtrsim 3 \text{ cm}^2/\text{g}^{-1}$ .

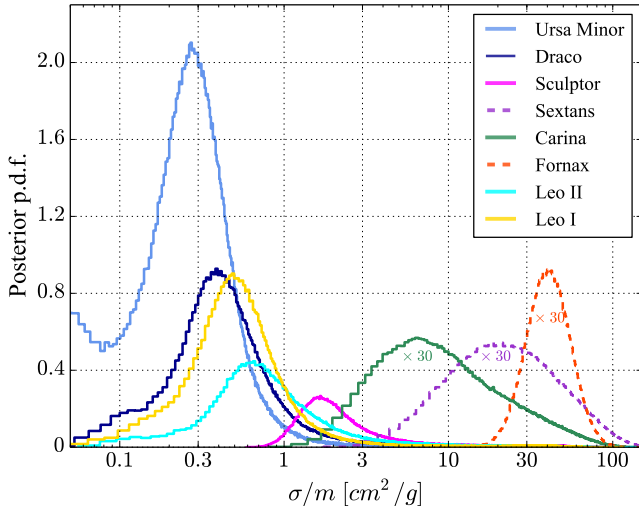


**Figure 3.** Posterior probability density function (p.d.f.) for the SIDM cross-section probed by MW classical dwarfs from our Bayesian fit. For the sake of readability, histograms for Sextans, Carina and Fornax are normalized to an area equal to 30 times unity. Note if both Fornax and Sextans are hosted by sub-halos less-massive than the 15 ones characterizing the spread of the gray band in figure 2, a smaller  $\sigma/m$  can be consistent with the data (Zavala et al. 2013).

We remark that such cross-section hierarchy matches the benchmark trends originally highlighted in SIDM-only simulations (Zavala et al. 2013; Elbert et al. 2015; Vogelsberger et al. 2016).

## 6. DISCUSSION.

In this work we have studied the TBTF problem for the brightest MW satellites in the context of SIDM. We show valuable fits of dSph kinematics within this model – along with stellar anisotropies from inner isotropic to outer radial orbits – in net contrast to the poor CDM-only predictions, see figure 1. Consistently with other astrophysical systems (Kaplinghat et al. 2016; Kamada et al. 2017), our data analysis of the brightest MW satellites point to SIDM cross-sections in the interval  $\sigma/m \sim 0.5 - 3 \text{ cm}^2\text{g}^{-1}$ , see figure 3. However, we also observe Sextans and Fornax probing cross-sections substantially larger, confirming trends from previous N-body studies (Zavala et al. 2013; Elbert et al. 2015). While  $\sigma/m$  values obtained here may depend on the assumed MW mass (Wang et al. 2012), the overall hierarchy depicted in figure 3 should not change. Environmental effects, such as the MW tidal field, may play an important role (Peñarrubia et al. 2010) and would need a better quantification within SIDM in light of the aforementioned two outlier objects. In this respect, we note that the methodology outlined here may be applied also to the TBTF problem in the field dwarfs (Ferrero et al. 2012; Garrison-Kimmel et al. 2014), possibly providing independent validation of the main results of this

work. We conclude observing that concrete realizations of the SIDM idea may present features, such as late kinetic decoupling (Bringmann et al. 2016) and dark acoustic damping (Cyr-Racine & Sigurdson 2013), not captured by our analysis, but potentially relevant for CDM small-scale puzzles (Vogelsberger et al. 2016). Model-building avenues along these directions may include peculiar astro-particle signatures (Bringmann et al. 2017; Huo et al. 2017), deserving further investigation.

*Acknowledgments:* M.V. acknowledges support from the European Research Council under the European Union’s Seventh Framework Programme (FP/2007-2013) / ERC Grant Agreements n. 279972 “NPFlavour”. H.B.Y. acknowledges support from U. S. Department of Energy under Grant No. de-sc0008541 and the Hellman Fellows Fund. Authors are grateful to Matthew Walker for providing the binned kinematics presented in Geringer-Sameth et al. (2015), acknowledge Peter Creasey, Manoj Kaplinghat, Mihael Petač, Laura Sales and Piero Ullio for useful discussions, and thank organizers and participants of the stimulating workshops “Self-Interacting Dark Matter” (Niels Bohr Institute), “WIMPs vs non-WIMPs in dwarf spheroidal galaxies” (University of Turin).

## REFERENCES

- J. S. Bullock and M. Boylan-Kolchin, *Ann. Rev. Astron. Astrophys.* **55**, 343 (2017), arXiv:1707.04256 [astro-ph.CO].
- S. Tulin and H.-B. Yu, (2017), arXiv:1705.02358 [hep-ph].
- A. A. Klypin, A. V. Kravtsov, O. Valenzuela, and F. Prada, *Astrophys. J.* **522**, 82 (1999), arXiv:astro-ph/9901240 [astro-ph].
- B. Moore, S. Ghigna, F. Governato, G. Lake, T. R. Quinn, J. Stadel, and P. Tozzi, *Astrophys. J.* **524**, L19 (1999), arXiv:astro-ph/9907411 [astro-ph].
- M. Boylan-Kolchin, J. S. Bullock, and M. Kaplinghat, *Mon. Not. Roy. Astron. Soc.* **415**, L40 (2011), arXiv:1103.0007 [astro-ph.CO].
- M. Boylan-Kolchin, J. S. Bullock, and M. Kaplinghat, *Mon. Not. Roy. Astron. Soc.* **422**, 1203 (2012), arXiv:1111.2048 [astro-ph.CO].
- A. Drlica-Wagner et al. (DES), *Astrophys. J.* **813**, 109 (2015), arXiv:1508.03622 [astro-ph.GA].
- M. G. Walker, M. Mateo, E. W. Olszewski, J. Peñarrubia, N. W. Evans, and G. Gilmore, *Astrophys. J.* **704**, 1274 (2009), [Erratum: *Astrophys. J.* 710, 886 (2010)], arXiv:0906.0341 [astro-ph.CO].
- J. Wolf, G. D. Martinez, J. S. Bullock, M. Kaplinghat, M. Geha, R. R. Munoz, J. D. Simon, and F. F. Avedo, *Mon. Not. Roy. Astron. Soc.* **406**, 1220 (2010), arXiv:0908.2995 [astro-ph.CO].
- T. Sawala et al., *Mon. Not. Roy. Astron. Soc.* **457**, 1931 (2016), arXiv:1511.01098 [astro-ph.GA].
- A. R. Wetzel, P. F. Hopkins, J.-h. Kim, C.-A. Faucher-Giguère, D. Kereš, and E. Quataert, *ApJL* **827**, L23 (2016), arXiv:1602.05957.
- A. Fattahi, J. F. Navarro, T. Sawala, C. S. Frenk, L. V. Sales, K. Oman, M. Schaller, and J. Wang (2016), arXiv:1607.06479.
- I. Ferrero, M. G. Abadi, J. F. Navarro, L. V. Sales, and S. Gurovich, *MNRAS* **425**, 2817 (2012), arXiv:1111.6609.

- J. Peñarrubia, A. Pontzen, M. G. Walker, and S. E. Koposov, *Astrophys. J.* **759**, L42 (2012), arXiv:1207.2772 [astro-ph.GA].
- S. Garrison-Kimmel, M. Rocha, M. Boylan-Kolchin, J. Bullock, and J. Lally, *Mon. Not. Roy. Astron. Soc.* **433**, 3539 (2013), arXiv:1301.3137 [astro-ph.CO].
- E. Papastergis, R. Giovanelli, M. P. Haynes, and F. Shankar, *Astron. Astrophys.* **574**, A113 (2015), arXiv:1407.4665 [astro-ph.GA].
- M. Vogelsberger, J. Zavala, F.-Y. Cyr-Racine, C. Pfrommer, T. Bringmann, and K. Sigurdson, *Mon. Not. Roy. Astron. Soc.* **460**, 1399 (2016), arXiv:1512.05349 [astro-ph.CO].
- D. N. Spergel and P. J. Steinhardt, *Phys. Rev. Lett.* **84**, 3760 (2000), arXiv:astro-ph/9909386 [astro-ph].
- M. Vogelsberger, J. Zavala, and A. Loeb, *Mon. Not. Roy. Astron. Soc.* **423**, 3740 (2012), arXiv:1201.5892 [astro-ph.CO].
- M. Rocha, A. H. G. Peter, J. S. Bullock, M. Kaplinghat, S. Garrison-Kimmel, J. Onorbe, and L. A. Moustakas, *Mon. Not. Roy. Astron. Soc.* **430**, 81 (2013), arXiv:1208.3025.
- M. Kaplinghat, R. E. Keeley, T. Linden, and H.-B. Yu, *Phys. Rev. Lett.* **113**, 021302 (2014), arXiv:1311.6524 [astro-ph.CO].
- O. D. Elbert, J. S. Bullock, S. Garrison-Kimmel, M. Rocha, J. Oorbe, and A. H. G. Peter, *Mon. Not. Roy. Astron. Soc.* **453**, 29 (2015), arXiv:1412.1477 [astro-ph.GA].
- A. Kamada, M. Kaplinghat, A. B. Pace, and H.-B. Yu, *Phys. Rev. Lett.* **119**, 111102 (2017), arXiv:1611.02716 [astro-ph.GA].
- P. Creasey, O. Sameie, L. V. Sales, H.-B. Yu, M. Vogelsberger, and J. Zavala, *Mon. Not. Roy. Astron. Soc.* **468**, 2283 (2017), arXiv:1612.03903 [astro-ph.GA].
- M. Kaplinghat, S. Tulin, and H.-B. Yu, *Phys. Rev. Lett.* **116**, 041302 (2016), arXiv:1508.03339 [astro-ph.CO].
- G. Battaglia, A. Helmi, E. Tolstoy, M. Irwin, V. Hill, and P. Jablonka, *Astrophys. J.* **681**, L13 (2008), arXiv:0802.4220 [astro-ph].
- J. H. An and N. W. Evans, *Astrophys. J.* **642**, 752 (2006), arXiv:0511686.
- J. An, E. Van Hese, and M. Baes, *Mon. Not. Roy. Astron. Soc.* **422**, 652 (2012), arXiv:1202.0004.
- N. C. Amorisco and N. W. Evans, *Mon. Not. Roy. Astron. Soc.* **419**, 184 (2012), arXiv:1106.1062 [astro-ph.CO].
- M. G. Walker and J. Peñarrubia, *Astrophys. J.* **742**, 20 (2011), arXiv:1108.2404 [astro-ph.CO].
- A. Agnello and N. W. Evans, *Astrophys. J.* **754**, L39 (2012), arXiv:1205.6673 [astro-ph.GA].
- N. C. Amorisco, A. Agnello, and N. W. Evans, *Mon. Not. Roy. Astron. Soc.* **429**, L89 (2013), arXiv:1210.3157 [astro-ph.CO].
- L. E. Strigari, C. S. Frenk, and S. D. M. White, *Astrophys. J.* **838**, 123 (2017), arXiv:1406.6079 [astro-ph.GA].
- G. Battaglia, A. Helmi, and M. Breddels, *New Astron. Rev.* **57**, 52 (2013), arXiv:1305.5965 [astro-ph.CO].
- J. F. Navarro, C. S. Frenk, and S. D. M. White, *Astrophys. J.* **490**, 493 (1997), arXiv:astro-ph/9611107 [astro-ph].
- A. Geringer-Sameth, S. M. Koushiappas, and M. Walker, *Astrophys. J.* **801**, 74 (2015), arXiv:0802.4220.
- M. Baes and E. Van Hese, *Astron. Astrophys.* **471**, 419 (2007), arXiv:0705.4109 [astro-ph].
- V. Bonnivard *et al.*, *Mon. Not. Roy. Astron. Soc.* **453**, 849 (2015), arXiv:1504.02048 [astro-ph.HE].
- A. W. McConnachie, *Astron. J.* **144**, 4 (2012), arXiv:1204.1562 [astro-ph.CO].
- D. Foreman-Mackey, D. W. Hogg, D. Lang, and J. Goodman, *Publ. Astron. Soc. Pac.* **125**, 306 (2013), arXiv:1202.3665.
- J. Goodman and J. Weare, *Comm. in App. Math. and Comp. Science* **5**, 65 (2010).
- P. Ullio and M. Valli, *JCAP* **1607**, 025 (2016), arXiv:1603.07721 [astro-ph.GA].
- J. Zavala, M. Vogelsberger, and M. G. Walker, *Mon. Not. Roy. Astron. Soc.* **431**, L20 (2013), arXiv:1211.6426.
- J. Wang, C. S. Frenk, J. F. Navarro, L. Gao, and T. Sawala, *MNRAS* **424**, 2715 (2012), arXiv:1203.4097 [astro-ph].
- J. Peñarrubia, A. J. Benson, M. G. Walker, G. Gilmore, A. W. McConnachie, and L. Mayer, *MNRAS* **406**, 1290 (2010), arXiv:1002.3376.
- S. Garrison-Kimmel, M. Boylan-Kolchin, J. S. Bullock, and E. N. Kirby, *MNRAS* **444**, 222 (2014), arXiv:1404.5313.
- T. Bringmann, H. T. Ihle, J. Kersten, and P. Walia, *Phys. Rev. D* **94**, 103529 (2016), arXiv:1603.04884 [hep-ph].
- F.-Y. Cyr-Racine and K. Sigurdson, *Phys. Rev. D* **87**, 103515 (2013), arXiv:1209.5752.
- T. Bringmann, F. Kahlhoefer, K. Schmidt-Hoberg, and P. Walia, *Phys. Rev. Lett.* **118**, 141802 (2017), arXiv:1612.00845.
- R. Huo, M. Kaplinghat, Z. Pan, and H.-B. Yu (2017), arXiv:1709.09717